



HAL
open science

Evidencing ((n-C₄H₉)(₄N)(₂)[W₆I₁₄] red-NIR emission and singlet oxygen generation by two photon absorption dagger

Yann Molard, Gregory Taupier, Serge Paofai, Stéphane Cordier

► To cite this version:

Yann Molard, Gregory Taupier, Serge Paofai, Stéphane Cordier. Evidencing ((n-C₄H₉)(₄N)(₂)[W₆I₁₄] red-NIR emission and singlet oxygen generation by two photon absorption dagger. *Chemical Communications*, 2021, 57 (33), pp.4003-4006. 10.1039/d1cc00751c . hal-03190420

HAL Id: hal-03190420

<https://hal.science/hal-03190420>

Submitted on 23 Apr 2021

HAL is a multi-disciplinary open access archive for the deposit and dissemination of scientific research documents, whether they are published or not. The documents may come from teaching and research institutions in France or abroad, or from public or private research centers.

L'archive ouverte pluridisciplinaire **HAL**, est destinée au dépôt et à la diffusion de documents scientifiques de niveau recherche, publiés ou non, émanant des établissements d'enseignement et de recherche français ou étrangers, des laboratoires publics ou privés.

Evidencing $((n\text{-C}_4\text{H}_9)_4\text{N})_2[\text{W}_6\text{I}_{14}]$ red-NIR emission and singlet oxygen generation by two photon absorption

Yann Molard,^{*a} Gregory Taupier,^a Serge Paofai^a and Stéphane Cordier^a

^a Université de Rennes, CNRS, ISCR - UMR 6226, ScanMAT – UMS 2001, F-35000 Rennes, France E-mail: yann.molard@univ-rennes1.fr.

Electronic Supplementary Information (ESI) available: [experimental procedures, time resolved photoluminescence studies, AQY measurements, 2PE spectra, singlet oxygen studies]. See DOI: 10.1039/x0xx00000x

We report the first proof of the ability of octahedral tungsten clusters to emit red-NIR light and to produce singlet oxygen upon two-photon absorption, in solution and in the solid-state. Such discoveries open new perspectives for tungsten cluster compounds in several fields like optoelectronic, photodynamic therapy, or bioimaging.

Known for about 90 years,¹ the two photon absorption (TPA) - induced luminescence is an active area of research in the field of three-dimensional optical data storage,² multiphoton emission spectroscopy and microscopy,³ or photodynamic therapy (PDT).⁴ In this last case, materials endowed with TPA-induced phosphorescence are particularly attractive. NIR excitation minimizes tissue autofluorescence and provides a deeper penetration in biological tissues compared to visible light. Besides, singlet oxygen can be produced by energy transfer from the triplet excited state reached by TPA. Hence, such materials are prime candidates for non-invasive therapy, and many of them have been developed using coordination complexes or organic compounds,⁵ quantum dots,⁶ rare earth⁷, and, more recently, carbon dots or silicon dots coupled to platinum group metals,⁸ or tetranuclear cubane-like Cu(I) compounds.⁹ Octahedral transition metal cluster compounds,¹⁰ of general formula $\text{A}_2\text{M}_6\text{X}_8\text{L}^3_6$ (A: cation, M: Mo or W, Xⁱ: halogen inner ligand, L^a: anionic apical ligand, **Figure 1a**) are obtained by solid state chemistry route or by combining solid state and solution chemistries. They are known for their abilities to emit in the red-NIR and produce singlet oxygen either upon UV-Vis irradiation or x-ray exposition.¹¹⁻¹⁵ Many studies have described their potential in cancer treatment,¹⁶⁻¹⁹ bioimaging,²⁰ optoelectronic,²¹⁻²⁴ lighting,^{25, 26} solar concentrator,^{27, 28} anticounterfeiting,²⁹ oxygen sensors³⁰⁻³³ or photocatalysis.³⁴ However, nothing is known about their potential in producing red-NIR light and singlet oxygen upon TPA. Herein, we demonstrate the first evidences of $((n\text{-C}_4\text{H}_9)_4\text{N})_2[\text{W}_6\text{I}_8\text{I}^a_6]$ (also written $((n\text{-C}_4\text{H}_9)_4\text{N})_2[\text{W}_6\text{I}_{14}]$) ability to emit red-NIR light and to generate singlet oxygen upon NIR excitation by TPA, enlarging its potentialities in the field of bioimaging and PDT. The tungsten cluster ternary salt was obtained following a reported procedure with conform analytical and structural data (see ESI for experimental details).³⁵

Emission measurements were realized in acetonitrile solution (aerated and deaerated) and on a powdered sample. First, one-photon absorption induced emission (1PE) and two-photon

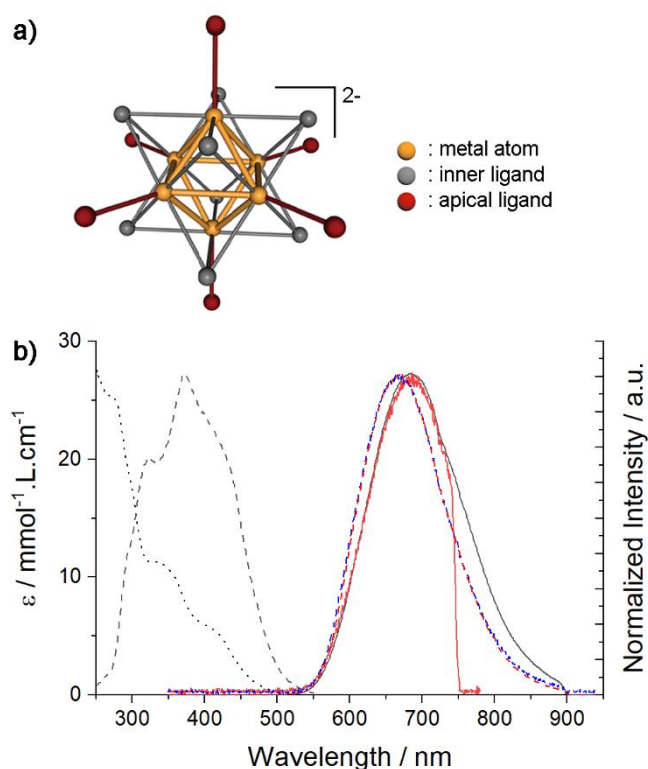


Figure 1. a) Schematic representation of the cluster anion; b) absorption (black dotted line), excitation (black dashed line, $\lambda_{\text{obs}}=680$ nm), normalized emission in solution for $\lambda_{\text{exc}} = 400$ nm (black solid line), $\lambda_{\text{exc}} = 810$ nm (red solid line) and, in the solid state for $\lambda_{\text{exc}} = 400$ nm (blue dashed line) and $\lambda_{\text{exc}} = 1010$ nm (red dashed line) spectra of $((n\text{-C}_4\text{H}_9)_4\text{N})_2[\text{W}_6\text{I}_{14}]$.

absorption induced emission (2PE) were investigated. **Figure 1b** presents the absorption and 1PE excitation spectra in solution as well as 1PE and 2PE emission spectra observed in solution and in the solid state. 1PE and 2PE spectra were recorded using the same set-up (Ti-sapphire femtosecond laser chain constituted by a Coherent Chameleon ultra II (pulse duration: 100-130 fs), a pulse picker (pulse frequency: 5MHz), a second harmonic generator, and an Ocean optics QEPro CCD detector, see ESI **figure S1** for the full set-up description) and are superimposable either in solution or in the solid state. $((n\text{-C}_4\text{H}_9)_4\text{N})_2[\text{W}_6\text{I}_{14}]$ emission is broad and structureless with a maximum position located at 668 or 682 nm in the solid state or in solution, respectively (**Table 1**). This shift is usual and reflects the influence of the environment on the cluster compound emission properties.³⁵

Such emission band is observed exciting the sample in solution from 280 nm up to more than 500 nm (dashed line, figure 1b). According to emission vs excitation maps (see ESI **Figure S2**), the excitation range is extended in the solid state from 250 nm up to 540 nm. Absolute quantum yield (AQY) were determined in air for the solid state and in aerated or deaerated solution. It is well known that, as phosphorescent emitters, the excited triplet state of octahedral clusters made of a Mo or W scaffold, transfers efficiently its energy to the ground triplet state of O₂ (³Σ_g⁻), thus generating the NIR emissive singlet oxygen O₂(¹Δ_g).^{19, 36-38} Hence, the AQY value of ((*n*-C₄H₉)₄N)₂[W₆I₁₄] passes from 0.02 in aerated CH₃CN to 0.35 in deaerated CH₃CN, while its excited state lifetime (τ) increases from 0.4 μs to 26.2 μs upon deaeration, values concordant with previously reported data (see ESI, Figures S3-S8 for emission decay map and integrated profiles).^{13, 38} In the solid state, as the experiment is realized in air, the excited state lifetime is significantly shorter (15.1 μs) than in deaerated solution. However, in these conditions, the cluster compound emits very efficiently as the AQY values calculated for an excitation ranging from 365 nm up to 485 nm, is higher than 0.8. Note that such values are nearly twice higher than the previously reported ones although the same set-up is used to measure it.^{13, 39} This could eventually be explained by differences in the methodology followed to prepare the solid sample (see ESI for explanations and Figure S9). Anyway, such high AQY, allowed us to observe 2PE up to an excitation at 1010 nm, which was not possible in solution (*vide infra*).

The Red-NIR cluster 2PE under NIR infrared excitation was examined at several wavelength: 810 nm (**Figure 2a**) and 850 nm in solution and 810, 950 and 1010 nm in the solid state (see ESI Figure S10-S11) and was confirmed, in all cases, by the quadratic dependence of the emission intensities with the excitation laser power. The two-photon absorption cross-section of ((*n*-C₄H₉)₄N)₂[W₆I₁₄] was evaluated in solution (**Figure 2b**) between 780 and 950 nm by using the following equation:

$$\sigma_2 = \frac{n c_{ref} F \Phi_{ref}}{n_{ref} c F_{ref} \Phi} \sigma_{2ref} \quad (1)$$

Where *ref* refers to a reference compound (Rhodamine B),⁴⁰ *n* are the refractive index of solvents, *c* the concentration, *F* the integrated intensity of the emission signal recorded in the same conditions, and Φ the emission quantum yield from single-photon excitation.⁴¹ Values are expressed in Göppert-Mayer unit (1 GM = 10⁻⁵⁰ cm⁴ s photon⁻¹) and are in the same range than values calculated for porphyrins or for the [Ru(bpy)₃]²⁺ complex.^{42, 43}

Although TPA cross section values might appear low compared to carefully engineered TPA emitters,⁴⁴⁻⁴⁷ we wish to state that the cluster structure has not yet been optimized to improve such parameter. Indeed, octahedral clusters can be easily functionalized with organic moieties either covalently by substitution of apical ligands^{48, 49} or *via* ionic assembling.²⁴ Grafting organic synthons able to improve clusters TPA cross-section should be the next step in this research field, like it has already been described *e.g.* for metalloporphyrins.⁵⁰ The production of singlet oxygen O₂ (¹Δ_g) by 1P absorption of W₆

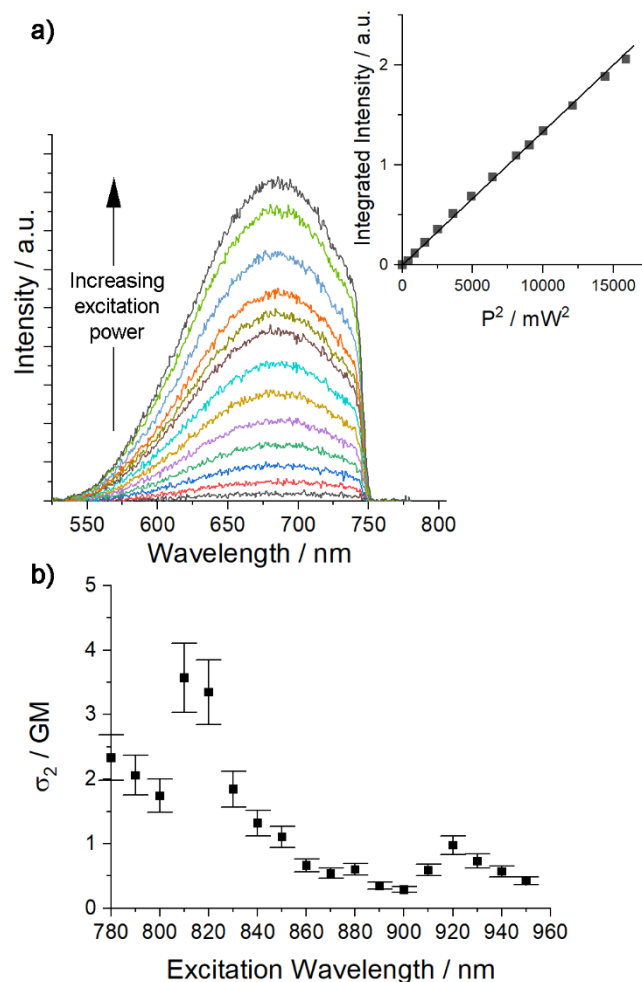


Figure 2. a) 2PE spectra vs irradiation power of ((*n*-C₄H₉)₄N)₂[W₆I₁₄] in deaerated CH₃CN ($\lambda_{exc} = 810$ nm, spectra are cut at 750 nm because of the optical filter used to prevent detector damages); inset: quadratic relationship of the observed two-photon emission intensity with the excitation laser power at 810 nm; b) two photon absorption cross section values vs excitation wavelength (1GM = 10⁻⁵⁰ cm⁴ s photon⁻¹); error on calculated values is estimated as $\pm 15\%$.

clusters is known for long,³⁶ and could be detected in aerated CH₃CN.

Table 1. Emission properties of ((*n*-C₄H₉)₄N)₂[W₆I₁₄] in solution and in the solid state: emission maximum position, 1PE excited state lifetime (τ) and 1PE absolute quantum yield (Φ).

	$\lambda_{max} / \text{nm}$		$\tau / \mu\text{s}$	Φ
	1PE $\lambda_{exc} = 405 \text{ nm}$	2PE $\lambda_{exc} = 810 \text{ nm}$		
solution	682	682	0.4	0.02
Solution deaerated ^[a]	682	682	26.2	0.35
powder	668	668	15.1	0.88

[a] deaeration is realized by bubbling Ar during 30 min.

Traces of O₂ (¹Δ_g) could also be detected by irradiating the solution at 810 nm (see ESI, Figure S11). This indicates that, despite low TPA cross-section values, the ((*n*-C₄H₉)₄N)₂[W₆I₁₄] cluster compound could act as an efficient singlet oxygen producer, of high interest for the development of TPA-induced PDT agent.

To conclude, we describe here the first evidences of two-photon absorption induced emission and singlet oxygen

production of an octahedral tungsten cluster compound, namely $((n-C_4H_9)_4N)_2[W_6I_{14}]$. Calculated 2PA cross-section values are in the same range than those of native porphyrin or ruthenium complexes. This work remains a proof of concept. Its next step will be to find a suitable way to increase the cluster 2PA cross section. This can be realized by associating the inorganic anion with 2PA antenna *via* electrostatic interactions or by apical ligand exchange. Our studies open new perspectives in the development of innovative tools for bioimaging and non-invasive PDT.

Notes and references

1. M. Göppert-Mayer, *Ann. Phys.*, 1931, **401**, 273-294.
2. K. Iliopoulos, O. Krupka, D. Gindre and M. Salle, *J. Am. Chem. Soc.*, 2010, **132**, 14343-14345.
3. V. Juvekar, S. J. Park, J. Yoon and H. M. Kim, *Coord. Chem. Rev.*, 2021, **427**, 213574.
4. G. Lemerrier, M. Four and S. Chevreux, *Coord. Chem. Rev.*, 2018, **368**, 1-12.
5. L. Xu, W. Lin, B. Huang, J. Zhang, X. Long, W. Zhang and Q. Zhang, *J. Mater. Chem. C*, 2021.
6. S.-C. Pu, M.-J. Yang, C.-C. Hsu, C.-W. Lai, C.-C. Hsieh, S. H. Lin, Y.-M. Cheng and P.-T. Chou, *Small*, 2006, **2**, 1308-1313.
7. H. Li, X. Wang, T. Y. Ohulchanskyy and G. Chen, *Adv. Mater.*, 2020, **n/a**, 2000678.
8. Y.-K. Dou, Y. Shang, X.-W. He, W.-Y. Li, Y.-H. Li and Y.-K. Zhang, *ACS Appl. Mater. Interfaces*, 2019, **11**, 13954-13963.
9. S.-Y. Yin, Z. Wang, Z.-M. Liu, H.-J. Yu, J.-H. Zhang, Y. Wang, R. Mao, M. Pan and C.-Y. Su, *Inorg. Chem.*, 2019, **58**, 10736-10742.
10. F. A. Cotton, *Inorg. Chem.*, 1964, **3**, 1217-1220.
11. M. A. Mikhaylov and M. N. Sokolov, *Eur. J. Inorg. Chem.*, 2019, 4181-4197.
12. B. Dierre, K. Costuas, N. Dumait, S. Paofai, M. Amela-Cortes, Y. Molard, F. Grasset, Y. Cho, K. Takahashi, N. Ohashi, T. Uchikoshi and S. Cordier, *Sci. Technol. Adv. Mater.*, 2017, **18**, 458-466.
13. D. V. Evtushok, A. R. Melnikov, N. A. Vorotnikova, Y. A. Vorotnikov, A. A. Ryadun, N. V. Kuratieva, K. V. Kozyr, N. R. Obedinskaya, E. I. Kretov, I. N. Novozhilov, Y. V. Mironov, D. V. Stass, O. A. Efremova and M. A. Shestopalov, *Dalton Trans.*, 2017, **46**, 11738-11747.
14. K. Kirakci, P. Kubát, K. Fejfarová, J. Martinčík, M. Nikl and K. Lang, *Inorg. Chem.*, 2016, **55**, 803-809.
15. A. W. Maverick, J. S. Najdzionek, D. MacKenzie, D. G. Nocera and H. B. Gray, *J. Am. Chem. Soc.*, 1983, **105**, 1878-1882.
16. N. Brandhonneur, Y. Boucaud, A. Verger, N. Dumait, Y. Molard, S. Cordier and G. Dollo, *Int. J. Pharm.*, 2021, **592**, 120079.
17. N. Brandhonneur, T. Hatahet, M. Amela-Cortes, Y. Molard, S. Cordier and G. Dollo, *Eur. J. Pharm. Biopharm.*, 2018, **125**, 95-105.
18. T. Hummel, D. Dutczak, A. Y. Alekseev, L. S. Adamenko, M. A. Shestopalov, Y. V. Mironov, D. Enseling, T. Jüstel and H.-J. Meyer, *RSC Adv.*, 2020, **10**, 22257-22263.
19. M. Bregnhøj, K. Strunge, R. J. Sørensen, M. Ströbele, T. Hummel, H. J. Meyer, F. Jensen and P. R. Ogilby, *J. Phys. Chem. A*, 2019, **123**, 1730-1739.
20. A. O. Solovieva, Y. A. Vorotnikov, K. E. Trifonova, O. A. Efremova, A. A. Krasilnikova, K. A. Brylev, E. V. Vorontsova, P. A. Avrorov, L. V. Shestopalova, A. F. Poveschenko, Y. V. Mironov and M. A. Shestopalov, *J. Mater. Chem. B*, 2016, **4**, 4839-4846.
21. N. Huby, J. Bignon, Q. Lagneaux, M. Amela-Cortes, A. Garreau, Y. Molard, J. Fade, A. Desert, E. Faulques, B. Beche, J.-L. Duvail and S. Cordier, *Opt. Mater.*, 2016, **52**, 196-202.
22. Y. Molard, C. Labbe, J. Cardin and S. Cordier, *Adv. Funct. Mater.*, 2013, **23**, 4821-4825.
23. S. M. Wood, M. Prevot, M. Amela-Cortes, S. Cordier, S. J. Elston, Y. Molard and S. M. Morris, *Adv. Opt. Mater.*, 2015, **3**, 1368-1372.
24. Y. Molard, *Acc. Chem. Res.*, 2016, **49**, 1514-1523.
25. E. Ferreira Molina, N. A. Martins de Jesus, S. Paofai, P. Hammer, M. Amela-Cortes, M. Robin, S. Cordier and Y. Molard, *Chem. Eur. J.*, 2019, **25**, 15248-15251.
26. M. Robin, N. Dumait, M. Amela-Cortes, C. Roiland, M. Harnois, E. Jacques, H. Folliot and Y. Molard, *Chem. Eur. J.*, 2018, **24**, 4825-4829.
27. S. Khelifi, J. Bignon, M. Amela-Cortes, N. Dumait, G. h. Loas, S. Cordier and Y. Molard, *ACS Appl. Mater. Interfaces*, 2020, **12**, 14400-14407.
28. Y. Zhao and R. R. Lunt, *Adv. Energy Mater.*, 2013, **3**, 1143-1148.
29. S. Khelifi, N. Fournier Le Ray, S. Paofai, M. Amela-Cortes, H. Akdas-Kilic, G. Taupier, S. Derien, S. Cordier, M. Achard and Y. Molard, *Mater. Today*, 2020, **35**, 34-41.
30. M. Amela-Cortes, S. Paofai, S. Cordier, H. Folliot and Y. Molard, *Chem. Commun.*, 2015, **51**, 8177-8180.
31. R. N. Ghosh, P. A. Askeland, S. Kramer and R. Loloee, *Appl. Phys. Lett.*, 2011, **98**, 221103/221101-221103/221103.
32. D. J. Osborn, III, G. L. Baker and R. N. Ghosh, *J. Sol-Gel Sci. Technol.*, 2005, **36**, 5-10.
33. R. N. Ghosh, G. L. Baker, C. Ruud and D. G. Nocera, *Appl. Phys. Lett.*, 1999, **75**, 2885-2887.
34. M. Feliz, P. Atienzar, M. Amela-Cortes, N. Dumait, P. Lemoine, Y. Molard and S. Cordier, *Inorg. Chem.*, 2019, **58**, 15443-15454.
35. M. N. Sokolov, K. A. Brylev, P. A. Abramov, M. R. Gallyamov, I. N. Novozhilov, N. Kitamura and M. A. Mikhaylov, *Eur. J. Inorg. Chem.*, 2017, 4131-4137.
36. J. A. Jackson, M. D. Newsham, C. Worsham and D. G. Nocera, *Chem. Mater.*, 1996, **8**, 558-564.
37. J. A. Jackson, C. Turro, M. D. Newsham and D. G. Nocera, *J. Phys. Chem.*, 1990, **94**, 4500.
38. T. C. Zietlow, D. G. Nocera and H. B. Gray, *Inorg. Chem.*, 1986, **25**, 1351-1353.
39. Y. A. Vorotnikov, M. A. Mikhailov, K. A. Brylev, D. A. Piryazev, N. V. Kuratieva, M. N. Sokolov, Y. V. Mironov and M. A. Shestopalov, *Russ. Chem. Bull.*, 2015, **64**, 2591-2596.
40. N. S. Makarov, M. Drobizhev and A. Rebane, *Opt. Express*, 2008, **16**, 4029-4047.
41. M. A. Albota, C. Xu and W. W. Webb, *Appl. Opt.*, 1998, **37**, 7352-7356.
42. F. N. Castellano, H. Malak, I. Gryczynski and J. R. Lakowicz, *Inorg. Chem.*, 1997, **36**, 5548-5551.
43. A. Karotki, M. Drobizhev, M. Kruk, C. Spangler, E. Nickel, N. Mamardashvili and A. Rebane, *J. Opt. Soc. Am. B*, 2003, **20**, 321-332.
44. M.-C. Yoon, S. B. Noh, A. Tsuda, Y. Nakamura, A. Osuka and D. Kim, *J. Am. Chem. Soc.*, 2007, **129**, 10080-10081.
45. T. Zhao, X. Shen, L. Li, Z. Guan, N. Gao, P. Yuan, S. Q. Yao, Q.-H. Xu and G. Q. Xu, *Nanoscale*, 2012, **4**, 7712-7719.
46. G. Ramakrishna, O. Varnavski, J. Kim, D. Lee and T. Goodson, *J. Am. Chem. Soc.*, 2008, **130**, 5032-5033.
47. R. Zhang, L. Yang, L. Kong, W. Hai-Yan, J.-X. Yang and X.-Y. Xu, *Optic. Mater.*, 2020, **106**, 109986.
48. L. F. Szczepura and E. Soto, in *Ligated Transition Metal Clusters in Solid-state Chemistry: The legacy of Marcel Sergent*, ed. J.-F. Halet, Springer International Publishing, Cham, 2019, pp. 75-108.
49. V. Cîrcu, Y. Molard, M. Amela-Cortes, A. Bentaleb, P. Barois, V. Dorcet and S. Cordier, *Angew. Chem. Int. Ed.*, 2015, **53**, 10921-10925.
50. O. S. Finikova, T. Troxler, A. Senes, W. F. DeGrado, R. M. Hochstrasser and S. A. Vinogradov, *J. Phys. Chem. A*, 2007, **111**, 6977-6990.

Electronic supplementary informations

Evidencing $((n\text{-C}_4\text{H}_9)_4\text{N})_2[\text{W}_6\text{I}_{14}]$ red-NIR emission and singlet oxygen generation by two photon absorption

Yann Molard,* Gregory Taupier, Serge Paofai and Stéphane Cordier

yann.molard@univ-rennes1.fr

Table of Contents

Table of Contents	4
Experimental Procedures	5
Synthesis and characterizations of $((n\text{-C}_4\text{H}_9)_4\text{N})_2[\text{W}_6\text{I}_{14}]$	5
Supplementary figures	6
Time resolved photoluminescence studies	7
AQY measurements	10
Two-photon emission spectra	10
Singlet oxygen generation studies	11
References	11

Experimental Procedures

Starting reagents were purchased from Alfa Aesar, Aldrich or Strem. EDX were realized in CMEBA-SCanMAT platform with a JED-2300 equipped with an EDS ITA300 (LA) spectrometer or with a JSM-7100F equipped with an Oxford X-Max spectrometer.

X-ray diffraction single crystal experiment. Suitable crystal for X-ray diffraction single crystal experiment were selected and mounted with a cryoloop on the goniometer head of a D8 Venture diffractometer diffractometer equipped with a (CMOS) PHOTON 100 detector, using Mo-K α radiation ($\lambda = 0.71073$ Å, multilayer monochromator) at T = 150(2) K.

Powder X-Ray diffraction experiments. X-Ray powder diffraction (XRPD) data were collected at room temperature using a Bruker D8 Advance two-circle diffractometer (θ - 2θ Bragg-Brentano mode) using Cu K α radiation ($\lambda = 1.54056$ Å) equipped with a Ge(111) monochromator and a Lynx Eye detector. The analyses of the diffraction patterns were performed using the FullProf and WinPlotr software packages.^[1]

All solvent used for photophysical measurements were of spectrometric grade. UV-vis absorption measurements, one photon emission vs excitation maps were recorded on a Horiba Jobin Yvon Duetta spectrophotometer. Deaeration of CH₃CN was realized by bubbling Ar in the solution for 30 min directly in the measuring cuvette. The absolute quantum yields were measured with a C9920-03 Hamamatsu system. One photon absorption lifetime measurements and TRPL mapping at 296 K were realized using a picosecond laser diode (Jobin Yvon deltadiode, 375 nm) and a Hamamatsu C10910-25 streak camera mounted with a slow single sweep unit. Signals were integrated on the whole emission decay. Fits were calculated using origin software and the goodness of fit judge by the reduced χ^2 value and residual plot shape.

Emission spectra by two photon or one photon absorption were recorded using a femtosecond laser chain (Ti-Sapphire Chameleon ultra II Coherent + pulse picker + SHG module when needed, pulse duration: 100-130 fs; pulse frequency: 5 MHz) and an Ocean optics QEPro CCD detector with integrating times ranging from 1 to 20s. The excitation beam crossed a lens before arriving on the sample and a short-pass 750 nm filter after the sample to remove the excitation signal and prevent damages on the CCD detector. The power of the beam was measured with a PMD100 console and a S142C integrating sphere sensor from Thorlabs. For solution measurements, the 2PE was recorded perpendicularly to the beam using an optical fiber connected to a CCD detector. Powder samples were deposited on a quartz substrate with an angle of 30° compared to the direction of the optical fiber.

Two-photon absorption cross-section values were evaluated using Rhodamine B as standard with a quantum yield value of 0.5^[2] (concentration: $8.12 \cdot 10^{-5}$ mol. l⁻¹ in MeOH) using σ_2 reference values from Makarov *et al.*^[3]

O₂ (¹ Δ_g) emission measurements were realized using either the picosecond laser diode at 375 nm for 1PE or the femtosecond laser chain for 2PE and detected with a Hamamatsu H12397-75 NIR-PMT unit mounted on an IHR3 spectrometer. In this las case, the excitation power was kept low enough to avoid any damages on the sample chamber mirrors.

Synthesis and characterizations of ((n-C₄H₉)₄N)₂[W₆I₈I^a₆]

((n-C₄H₉)₄N)₂[W₆I₈I^a₆] was prepared according to protocols reported in the literature. The synthesis is realized in three steps:

1) W₆Cl₁₂ was synthesized by a multistep reaction from the reduction of WCl₆ (Strem, 99.9%) by metal bismuth (Strem, 99.9%) in a sealed silica container. The extraction of [W₆Cl₈Cl^a₆]²⁻ units was performed in HCl acidic solution and lead to the formation of crystalline chloro acid (H₃O)₂[W₆(μ_3 -Cl)₈Cl₆](OH)_x that was thermally decomposed at 400°C under vacuum in W₆Cl₁₂.^[4]

2) [W₆I₈I^a₆]²⁻ cluster units were formed by ligand exchange and excision reaction by reacting at 540° for 15 min, in a sealed silica container, the binary W₆Cl₁₂ with a 10-fold excess (i.e. moles of I⁻ per mole of Cl⁻) of a molten solution of KI (Alfa Aesar, 99.9%) and Lil (Alfa Aesar, 99.9%) (70:30 mol %).^[5]

3) the resulting crude product was dissolved in ethanol. ((n-C₄H₉)₄N)₂[W₆I₈I^a₆] was obtained as a precipitate by addition in the solution of a 2 fold excess of (n-C₄H₉)₄Nl (Aldrich >99%) per [W₆I₈I^a₆]²⁻.^[6] After washing with ethanol and drying at 60°C in an oven, the ((n-C₄H₉)₄N)₂[W₆I₈I^a₆] precipitate was dissolved in CH₂Cl₂. Single crystals, with size ranging from 0.1 mm to 0.9 mm, were obtained by slow solvent evaporation.

The single crystal X-ray diffraction studies revealed the same structure for ((n-C₄H₉)₄N)₂[W₆I₈I^a₆] obtained herein than that reported by T.C. Zietlow *et al.* (Space group P2₁/n (No. 14), a = 11.553 (7) Å, b = 11.486 (3)Å, c = 24.554 (13) Å, $\beta = 96.77$ (4)°).^[7] More recently L. Riehl *et al.* reported the same structure using X-ray powder investigations (space group P2₁/n (No. 14), a = 11.5768(2) Å, b = 11.4916(3)Å, c = 24.5672(5) Å, $\beta = 96.776$ (2)°).^[8] Briefly, this structure is built up from [W₆I₈I^a₆]²⁻ discrete cluster units. The charge of the [W₆I₈I^a₆]²⁻ dianion is counterbalanced by two (C₄H₉)₄N⁺ cations. Within the structure, layers of clusters units alternate with layers of (C₄H₉)₄N⁺ along the c direction of the unit cell. EDS analysis of heavy atoms agreed with a W: I ratio of 6:14, with no trace of other heavy atom. A powdered sample of ((n-C₄H₉)₄N)₂[W₆I₈I^a₆] was obtained by grounding 300 mg of single-crystals. X-ray powder pattern of grounded single crystals, as expected, did not revealed the presence of any impurities or the presence of allotropic forms. Optical analyses were then performed on this pure powdered sample.

Supplementary figures

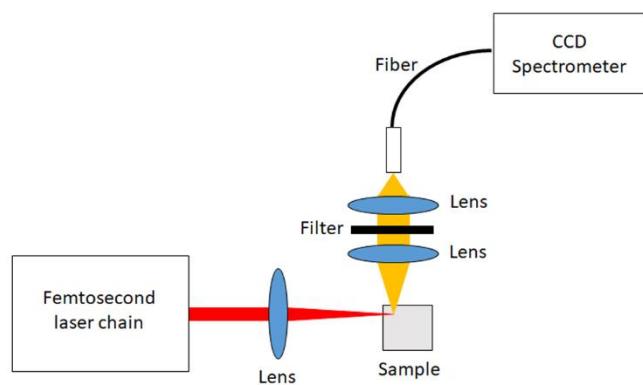


Figure S1. Schematic presentation of the photophysical set-up used for two photon absorption induced emission measurements in solution.

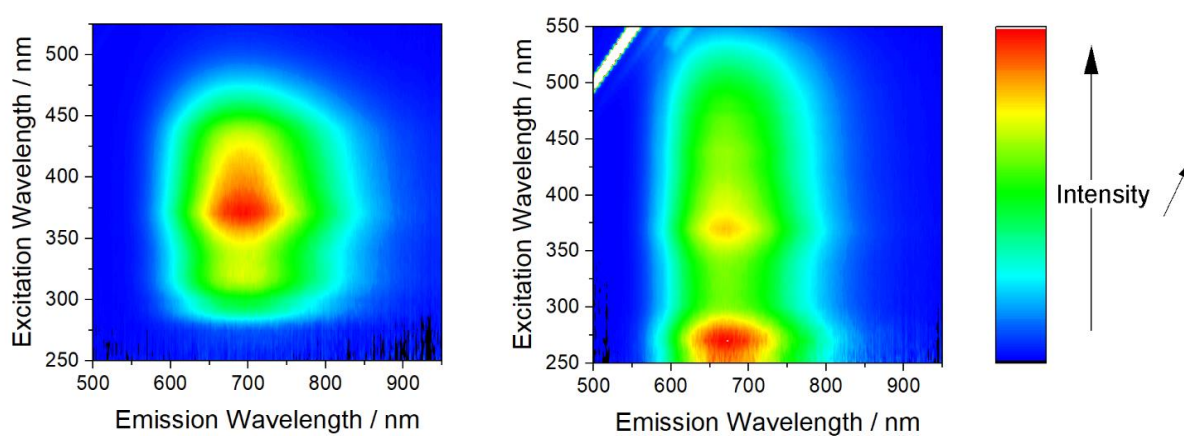


Figure S2. Emission vs excitation map of $((n\text{-C}_4\text{H}_9)_4\text{N})_2[\text{W}_6\text{I}_{14}]$ in CH₃CN (left) and in the solid state (right)

Time resolved photoluminescence studies

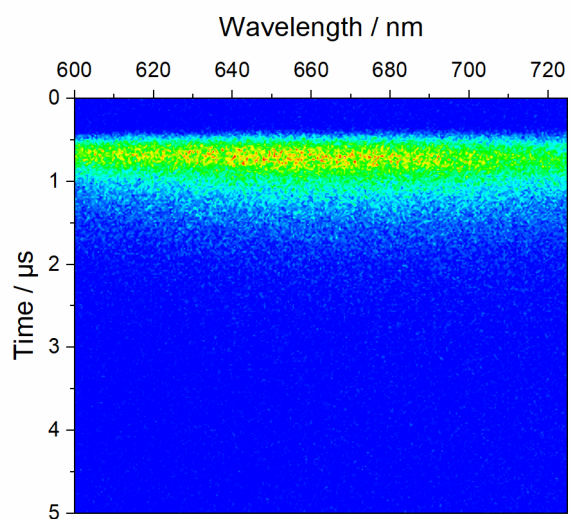


Figure S3. Emission decay map of $((n\text{-C}_4\text{H}_9)_4\text{N})_2[\text{W}_6\text{I}_{14}]$ in aerated CH_3CN

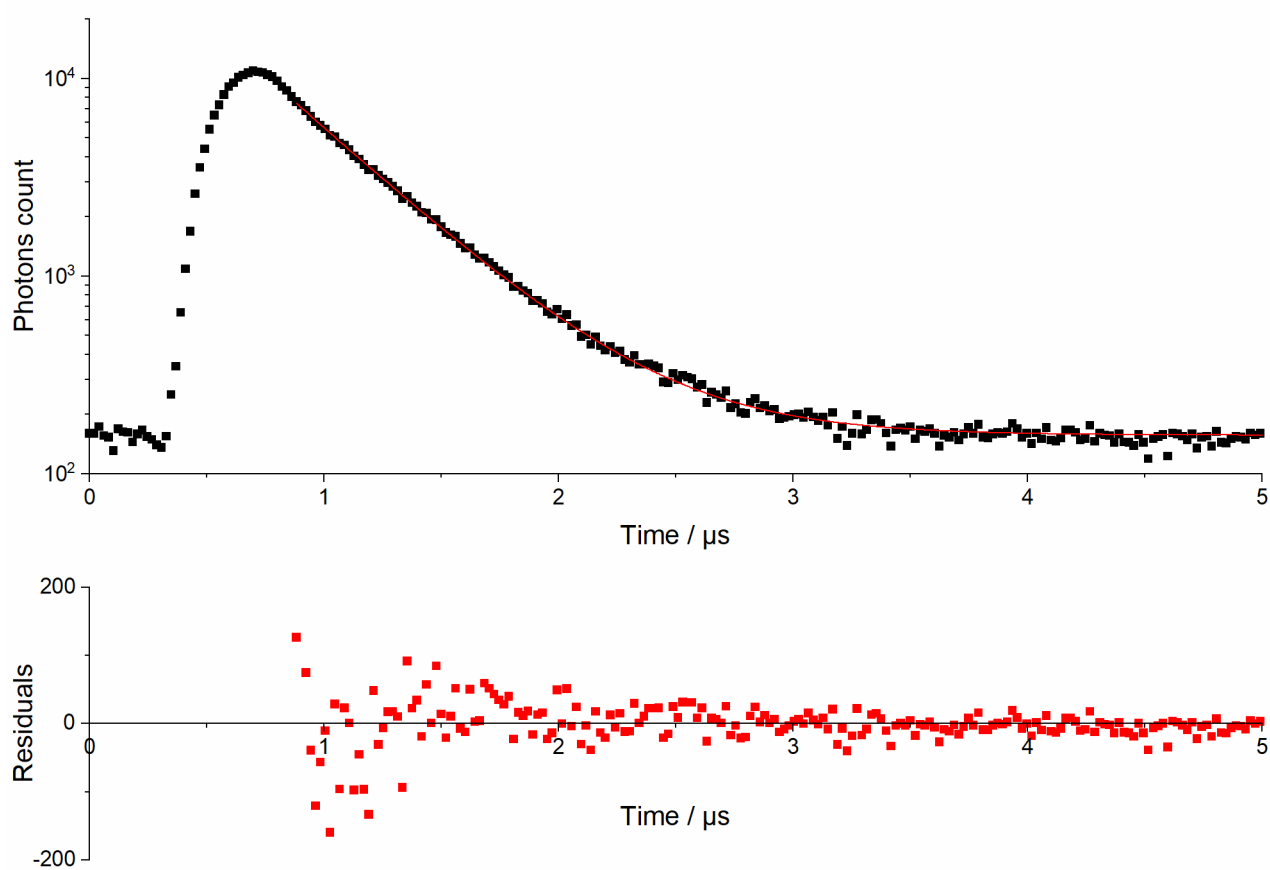


Figure S4. Integrated emission decay profile of $((n\text{-C}_4\text{H}_9)_4\text{N})_2[\text{W}_6\text{I}_{14}]$ in aerated CH_3CN

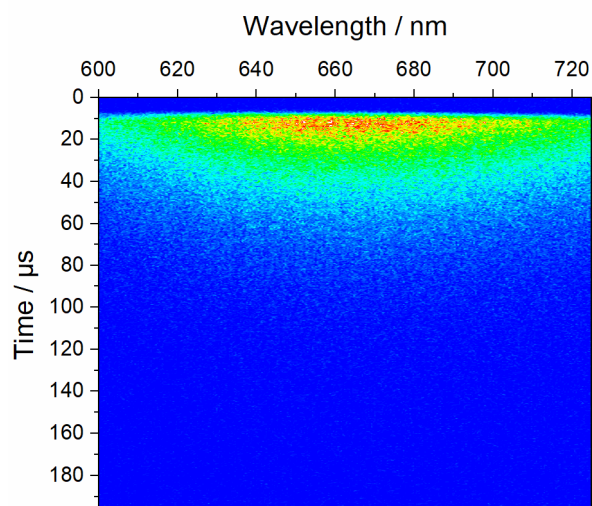


Figure S5. Emission decay map of $((n\text{-C}_4\text{H}_9)_4\text{N})_2[\text{W}_6\text{I}_{14}]$ in deaerated CH_3CN

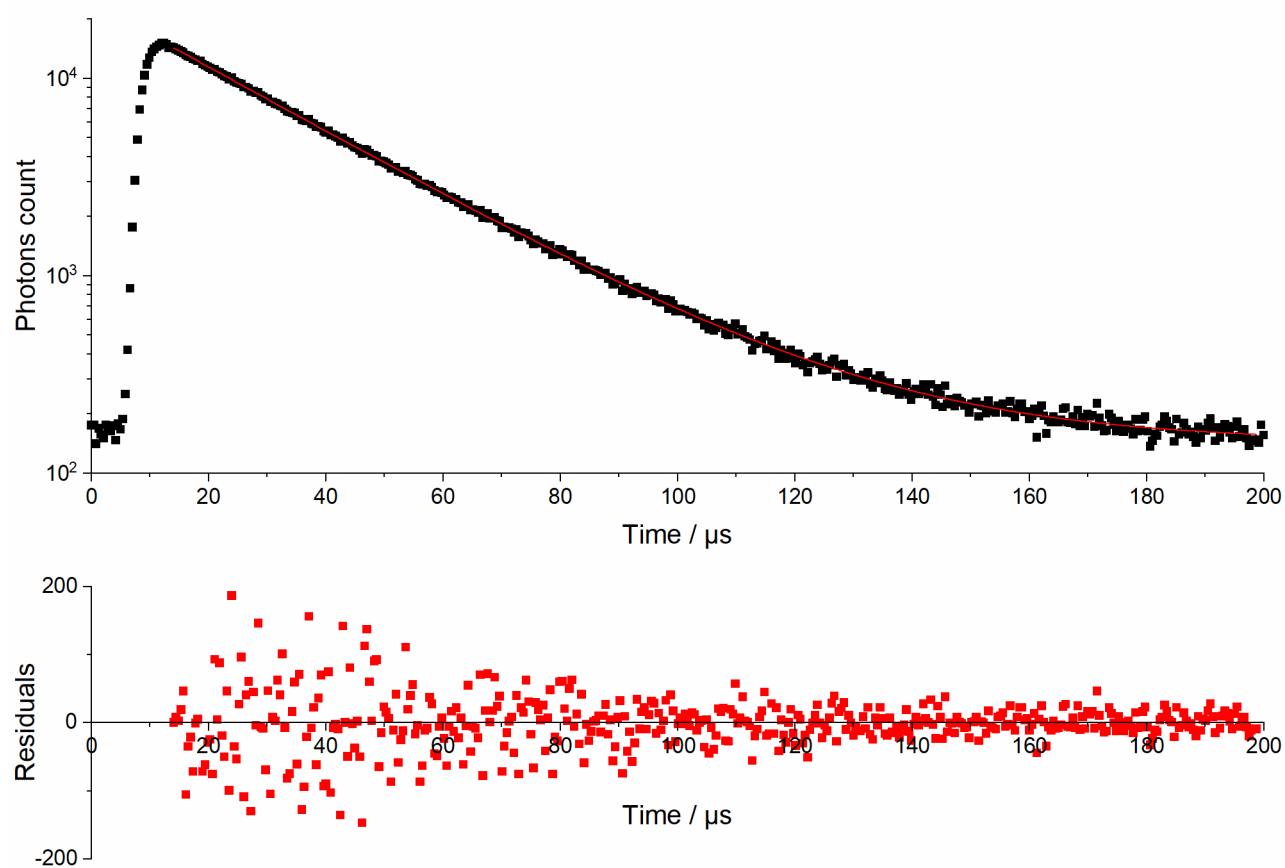


Figure S6. Integrated emission decay profile of $((n\text{-C}_4\text{H}_9)_4\text{N})_2[\text{W}_6\text{I}_{14}]$ in deaerated CH_3CN

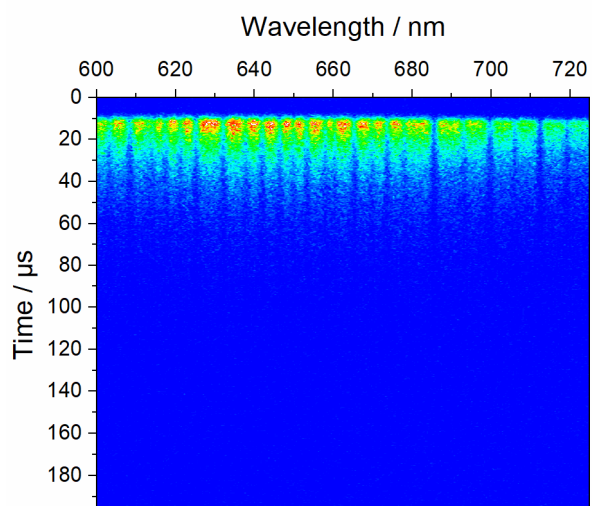


Figure S7. Emission decay map of $((n\text{-C}_4\text{H}_9)_4\text{N})_2[\text{W}_6\text{I}_{14}]$ in the solid state

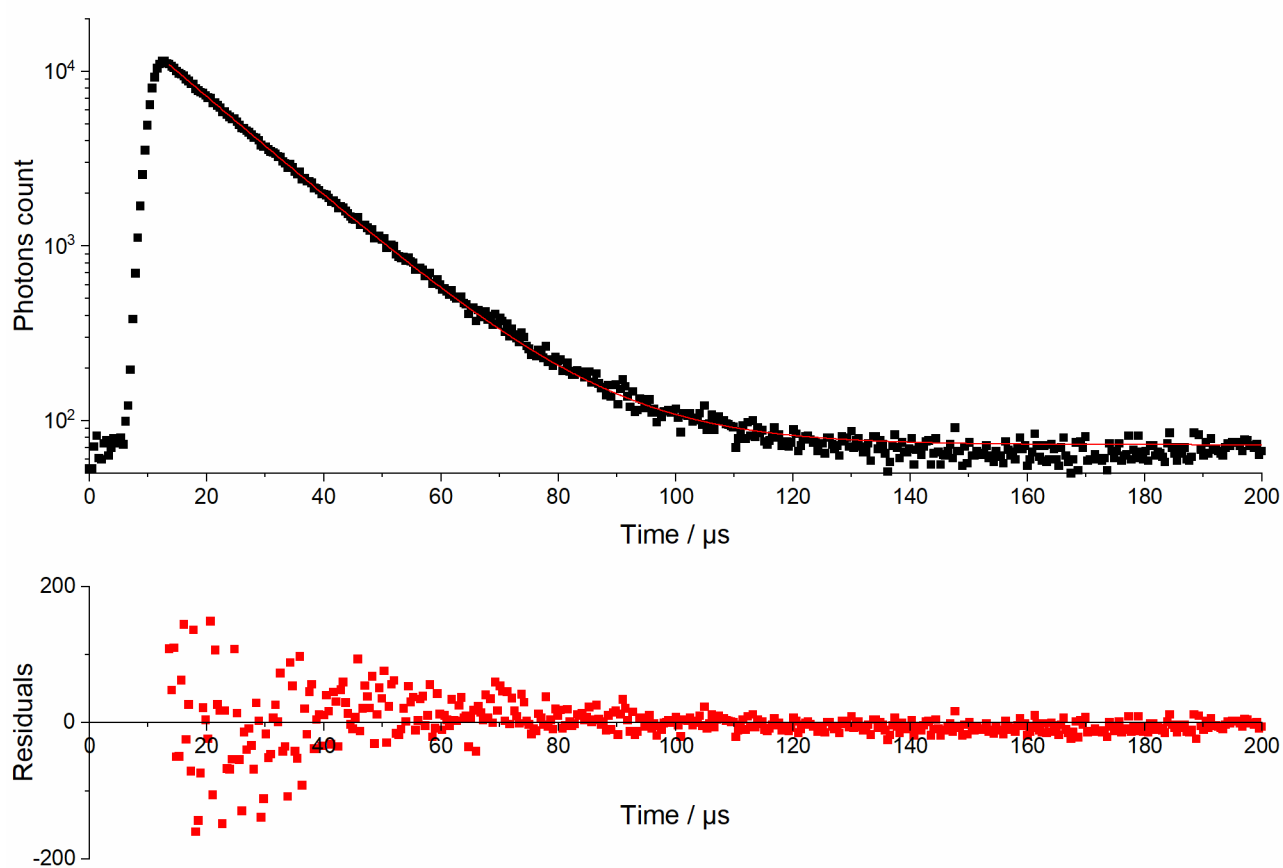


Figure S8. Integrated emission decay profile of $((n\text{-C}_4\text{H}_9)_4\text{N})_2[\text{W}_6\text{I}_{14}]$ in the solid state

AQY measurements

The absolute quantum yields were measured with a C9920–03 Hamamatsu system. Such system is composed by an excitation source, a monochromator, an integrating sphere and a Hamamatsu PMA12 CCD detector.

Samples are prepared as follow: a tiny amount of powder is deposited inside the quartz cuvette so that the percentage of absorbed excitation light is kept around 60% (according to the manufacturer, a minimal absorption of 50% is mandatory to generate accurate results). Using such tiny amount allows all the emitted light to be collected in a 4π solid angle inside the integrating sphere, which cannot be the case if the cuvette is fully filled in.

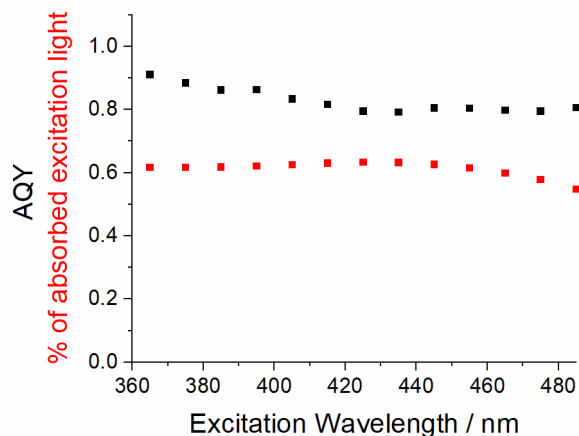


Figure S9. Calculated AQY values (black) and percentage of absorbed excitation light (red) used for the calculation for wavelengths ranging from 365 nm up to 485 nm. Uncertainty is around 10%.

Two-photon emission spectra

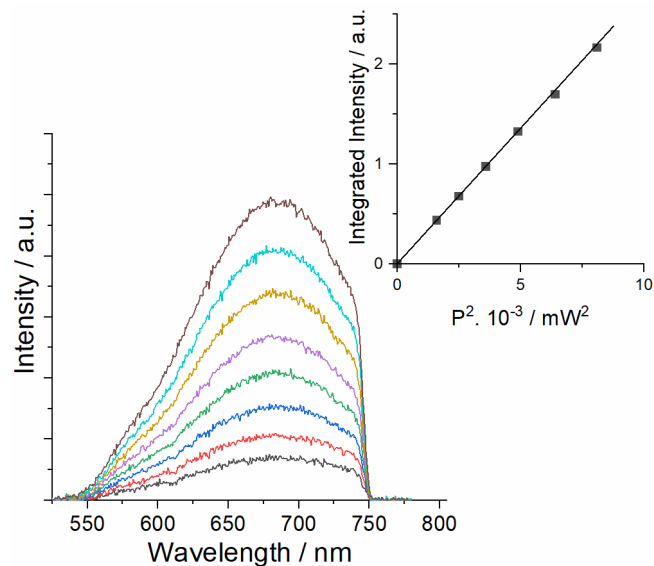


Figure S10. 2PE spectra vs irradiation power of a) $((n\text{-C}_4\text{H}_9)_4\text{N})_2[\text{W}_6\text{I}_{14}]$ in deaerated CH_3CN (spectra are cut at 750 nm because of the optical filter used to prevent detector damages); inset: quadratic relationship of the observed two-photon emission intensity with the excitation laser power at 850 nm.

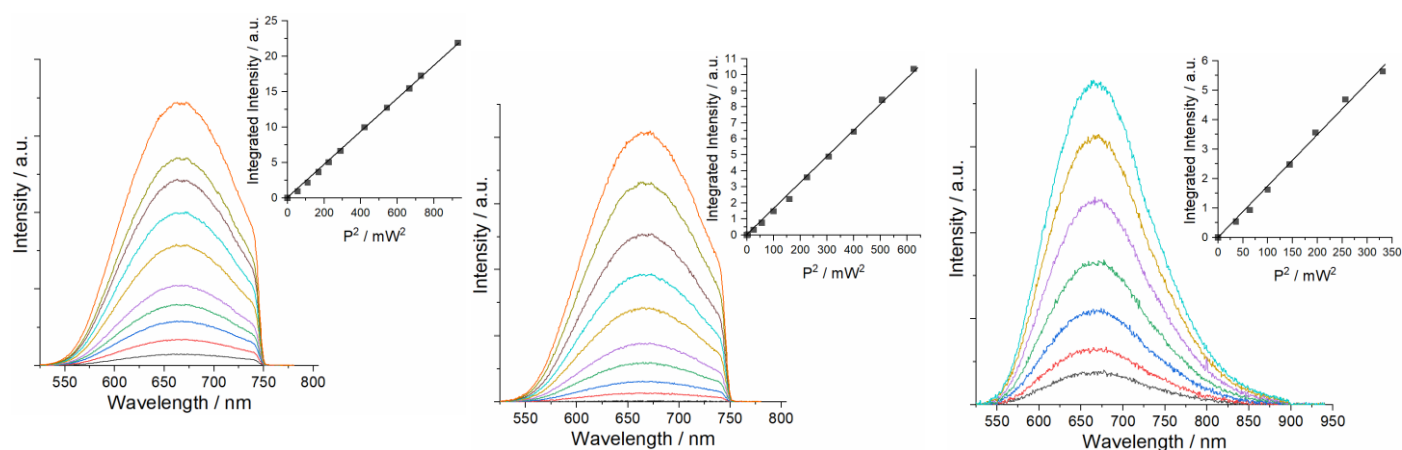


Figure S11. 2PE spectra vs irradiation power of $((n\text{-C}_4\text{H}_9)_4\text{N})_2[\text{W}_6\text{I}_{14}]$ in the solid state (spectra are cut at 750 nm because of the optical filter used to prevent detector damages); inset: quadratic relationship of the observed two-photon emission intensity with the excitation laser power. Excitation at 810 nm (left), 950 nm (middle) and 1010 nm (right).

Singlet oxygen generation studies

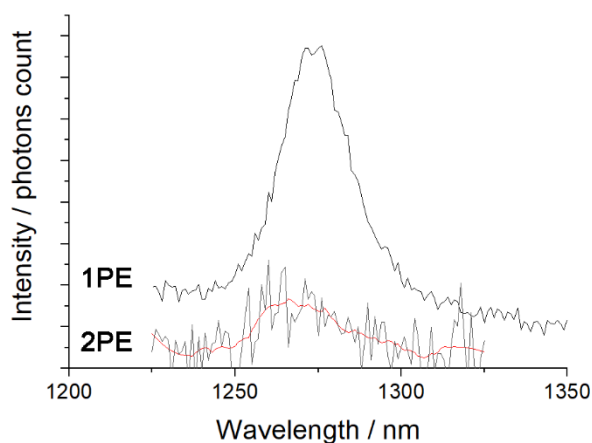


Figure S12. Singlet oxygen $\text{O}_2(a^1\Delta_g)$ emission spectra observed in aerated CH_3CN upon $((n\text{-C}_4\text{H}_9)_4\text{N})_2[\text{W}_6\text{I}_{14}]$ excitation at 375 nm (1PE) and 810 nm (2PE, the red curve is obtained by smoothing experimental data).

References

- [1] a) J. Rodríguez-Carvajal, *Physica B* **1993**, 192, 55-69; b) T. Roisnel, J. Rodríguez-Carvajal, *Mater. Sci. Forum* **2001**, 378-381, 118-123.
- [2] O. S. Finikova, T. Troxler, A. Senes, W. F. DeGrado, R. M. Hochstrasser, S. A. Vinogradov, *J. Phys. Chem. A* **2007**, 111, 6977-6990.
- [3] N. S. Makarov, M. Drobizhev, A. Rebane, *Opt. Express* **2008**, 16, 4029-4047.
- [4] V. Kolesnichenko, L. Messerle, *Inorg. Chem.* **1998**, 37, 3660-3663.
- [5] R. D. Hogue, R. E. McCarley, *Inorg. Chem.* **1970**, 9, 1354-1360.
- [6] M. N. Sokolov, K. A. Brylev, P. A. Abramov, M. R. Gallyamov, I. N. Novozhilov, N. Kitamura, M. A. Mikhaylov, *Eur. J. Inorg. Chem.* **2017**, 2017, 4131-4137.
- [7] T. C. Zietlow, D. G. Nocera, H. B. Gray, *Inorg. Chem.* **1986**, 25, 1351-1353.
- [8] L. Riehl, A. Seyboldt, M. Ströbele, D. Ensling, T. Jüstel, M. Westberg, P. R. Ogilby, H. J. Meyer, *Dalton Trans* **2016**, 45, 15500.